First-principles study on anatase TiO_2 codoped with nitrogen and praseodymium*

Gao Pan(高 攀), Wu Jing(吴 晶),
Liu Qing-Ju(柳清菊)†, and Zhou Wen-Fang(周文芳)

Yunnan Key Laboratory of Nanomaterials & Technology, Yunnan University, Kunming 650091, *China*

(Received 9 December 2009; revised manuscript received 2 February 2010)

The crystal structures, electronic structures and optical properties of nitrogen or/and praseodymium doped anatase TiO_2 were calculated by first principles with the plane-wave ultrasoft pseudopotential method based on density functional theory. Highly efficient visible-light-induced nitrogen or/and praseodymium doped anatase TiO_2 nanocrystal photocatalyst were synthesized by a microwave chemical method. The calculated results show that the photocatalytic activity of TiO_2 can be enhanced by N doping or Pr doping, and can be further enhanced by N+Pr codoping. The band gap change of the codoping TiO_2 is more obvious than that of the single ion doping, which results in the red shift of the optical absorption edges. The results are of great significance for the understanding and further development of visible-light response high activity modified TiO_2 photocatalyst. The photocatalytic activity of the samples for methyl blue degradation was investigated under the irradiation of fluorescent light. The experimental results show that the codoping TiO_2 photocatalytic activity is obviously higher than that of the single ion doping. The experimental results accord with the calculated results.

Keywords: nitrogen and praseodymium codoping, TiO_2 photocatalyst, microwave chemical method

PACC: 7115M, 7115H, 7115A

1. Introduction

As a photocatalytic material, TiO_2, owning to its nontoxicity, low cost, chemical stability, has been used in many fields such as solar cells, air and water pollution controlling and self-cleaning. It is the most potential photocatalyst. However, as a wide band gap oxide semiconductor ($E_g = 3.23$ eV), anatase TiO_2 only shows photocatalytic activity under UV-light irradiation ($\lambda < 384$ nm) that accounts for only a small fraction ($\sim$5%) of the solar energy, so its solar energy utilization is very low. Furthermore, its photo quantum yield is also very low due to its photoexcited electron–hole pairs recombining easily. Therefore, narrowing the band gap and reducing the recombination rate of photoexcited electron–hole pairs is an effective approach to improve the photocatalytic activity of TiO_2. Recently, many attempts have been made to improve TiO_2 photocatalytic performance under visible-light irradiation, such as ion-doping,[1−3] noble metal loading,[4] semiconductor compounding[5] and dye sensitizing.[6] Among these modification methods, ion doping is considered as one of the most effective methods.

The previous research has mostly concentrated on the single ion-doping into TiO_2,[7,8] but a few latest researches show that, compared with single ion-doping, different ion co-doping TiO_2 can further enhance its optical absorption range and photocatalytic activity because of the synergistic reaction. Xu *et al.*[9] prepared Eu and N codoping TiO_2 nanoparticles, the results showed that the codoped photocatalysts exhibit smaller spherical shape particles, the absorbance spectra show a significant red shift to the visible region, and the photocatalytic activity is highly improved compared with that of N-doped TiO_2 and pure TiO_2. Liu *et al.*[10] synthesized the metal and nitrogen codoping TiO_2 photocatalysts, they found that the codoping TiO_2 has a highly photo-response for visible-light, and the radius and alterable valence states of doping metallic cations play important roles on their photocatalytic activity.

Experimental studies of ions codoping TiO_2 have achieved some results, but there is still much con-

*Project supported by the National Natural Science Foundation of China (Grant No. 50862009), the New Century Excellent Talents in University of the Ministry of Education, China (Grant No. NCET-04-0915), and the Natural Science Foundation of Yunnan Province of China (Grant No. 2005E007M).

†Corresponding author. E-mail: qjliu@ynu.edu.cn

© 2010 Chinese Physical Society and IOP Publishing Ltd

troversy on the modification mechanism of ion doping TiO_2 due to widely varying experimental conditions, sample preparations, the determination of photo-reactivity, and the lack of detailed information about effects of ion doping on electronic structure of TiO_2. In contrast to experimental investigations, the theoretical analysis by computer simulation could overcome effects of complex experimental factors and clarify the ion doping effects on crystal structure and electronic structure. Mi Lan *et al.*[11] calculated N and H codoping effect on TiO_2 electronic structure, the results showed that N 2p states above the valence band (VB) are sufficiently mixed with the O 2p states in the VB, the continuum mixed states shifted the valence band maximum (VBM) upwards, narrowed the band gap, and consequently shifted the optical absorption edge to the visible-light region. Zhao *et al.*[12] investigated the effects of N and V codoping on the crystal structure, electronic structure and optical properties, the calculated results showed that N and V codoping can effectively red-shift the optical absorption edge of the TiO_2, which simultaneously has shallow acceptor and shallow donor in the band gap, and has local internal fields, which enable photoexcited electron–hole pairs separation become easier; the band edge is slightly changed by codoping, so it has stronger redox potential than that of pure TiO_2.

In particular, because of the unique 4f electronic configuration and spectral characteristics, lanthanides are ideal dopants for modifying the crystal structure, electronic structure, optical properties of TiO_2. On the other hand, the mixing of N 2p states with O 2p states and Ti 3d broadens the width of VB, and the band gap of TiO_2 is narrowed, therefore TiO_2 has the ability to absorb visible light. In order to further investigate the modification mechanism of anatase TiO_2 doped with N and Pr, the plane-wave ultrasoft pseudopotential method within the framework of the first-principles has been used to calculate the crystal structure, electronic structure and optical properties of N+Pr doping, and by comparing with N doping, Pr doping and pure TiO_2, we could clarify how these ions impact the photocatalytic activity of TiO_2.

2. Calculation and experimental methods

Anatase TiO_2 has a tetragonal structure (space group: $I4_1/amd$, local symmetry: D_{4h}^{19}) and contains four Ti atoms and eight O atoms in the conventional cell. Our models ($2\times2\times1$ supercell) consisted of four conventional cells stacked along the a-axes and b-axes, as shown in Fig. 1. In N+Pr doped TiO_2 model, a Ti atom was substituted by a Pr atom and an O atom was substituted by an N atom. Thus, one supercell consisted of 15 Ti atoms, 31 O atoms, one Pr atom and one N atom. The atomic concentration of impurity was about 2.08% (atomic fraction) in total. The other models are created by the same method.

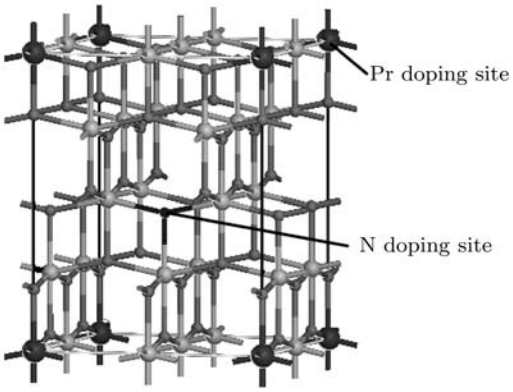


Fig. 1. Supercell model of N+Pr-doped anatase TiO_2 in the present work and the site of dopants.

All calculations were performed with the CASTEP module in Materials Studio 4.0 developed by Accelrys Software Inc. CASTEP is the first principle quantum mechanical process based on the density functional theory (DFT). It uses a total energy plane-wave pseudopotential method. The wave functions of valence electrons are expanded by using a planewave basis set within a specified energy cutoff chosen as 380 eV. The electronic exchange–correlation energy is treated within the framework of the local density approximation (LDA). The core electrons are replaced by the ultrasoft core potentials, and the valence atomic configurations are $3s^23p^63d^24s^2$ for Ti, $2s^22p^4$ for O, $2s^22p^3$ for N and $4f^3\ 5s^2\ 5p^6\ 6s^2$ for Pr in the calculation. The Monkhorst–Pack scheme K-points grid sampling was set as 3×7×3 for the irreducible Brillouim zone. A 45×24×54 mesh was used for fast Fourier transformation. The convergences were set as 5×10^{-4} Å (1 Å = 0.1 nm) for maximum displacement tolerances, 0.1 eV/nm for maximum force, 0.02 GPa for maximum stress and 5×10^{-6} eV/atom for total energy change in the geometry optimization.

To get accurate results, we first optimized the crystal structures and atomic coordinates, by minimizing the total energy and atomic forces. In our

calculations, the cell parameters had optimized during the geometry optimization, in addition to atomic coordinations, by performing an iterative process in which the coordinates of the atoms and the cell parameters are adjusted so that the total energy of the structure is minimized. Thus we could obtain stable structures for all models. Then we calculated the electronic structures and optical properties of the optimized supercells.

During the experimental process, an appropriate amount of $Ti(OC_4H_9)_4$ and hydrolysis inhibitor (prepared by our group) were added into distilled water at a certain temperature. By adjusting the pH with HNO_3, solution A was got. And solution B was got by completely dissolving a certain amount of $Pr(NO_3)_3{\cdot}6H_2O$ in distilled water. Then solution B was slowly dropped into solution A, keeping stirring for a certain time, the Pr–TiO_2 sols were obtained. After a certain proportion of urea as the nitrogen source was added into the sols, the sols were put into the microwave reactor for synthesizing, and then dried, heat-treated at an appropriate temperature. Finally the N+Pr–TiO_2 was obtained.

3. Results and discussion

3.1. Crystal structure

By optimizing the pure anatase TiO_2 supercell, we obtained the lattice parameters as follows: $a = b = 3.7431$ Å, $c = 9.4812$ Å, $d_{ap} = 1.9698$ Å, $d_{eq} = 1.9141$ Å, $2\theta = 155.840°$. They are in good agreement with the experimental results:[13] $a = b = 3.7848$ Å, $c = 9.5124$ Å, $d_{ap} = 1.9799$ Å, $d_{eq} = 1.9338$ Å, $2\theta = 156.233°$. The result implies that our calculation methods are reasonable, and the calculated results are authentic.

We analysed the relatively difficult degree for different ions doping into anatase TiO_2 by impurity formation energies, which is a widely accepted method. In this work, the impurity formation energy is defined as the following formula:[14]

$$E_f = E_{TiO_2:D} - E_{TiO_2} - \frac{1}{2}E_{N_2} - E_{Pr} + \frac{1}{2}E_{O_2} + E_{Ti}, \quad (1)$$

where $E_{TiO_2:D}$ and E_{TiO_2} are the total energies of N+Pr-doped TiO_2 and pure TiO_2 in the supercell with same size. E_{N_2} and E_{O_2} are the energies of N_2 and O_2 gas molecules, E_{Pr} and E_{Ti} are the energies of bulk Pr and Ti metal, respectively. The calculated results are shown in Table 1. According to the results, we find that the E_f of N+Pr-doped TiO_2 is larger than that of the others. In consequence, the synthesis of the N+Pr-doped TiO_2 becomes relatively difficult. And also the lattice distortions, average bond lengths, average net charges by Mulliken population analysis and average octahedral dipole moments in different ions doped anatase TiO_2 by geometry optimizing are given in Table 1. The changes of cell volume, bond length and charge on atoms result in that the centre of the gravity of negative electric charges is deviated from the position of Ti^{4+} ion in TiO_6 octahedron and its dipole moment is not zero. Sato *et al.*[15] reported that the local internal fields due to the dipole moment of distorted octahedral can promote the charges separation in the initial process of photoexcitation, and are useful for enhancing photocatalytic activity. According to Table 1, N doping or Pr doping can greatly enhance the photocatalytic activity of TiO_2. This conclusion is consistent with the results in recent literatures.[16,17] For N+Pr-doped TiO_2, these changes are more obvious than that of single ion doping TiO_2. This means that N+Pr doping can further enhance the photocatalytic activity of TiO_2 comparing with single ion doping.

Table 1. Formation energies, lattice distortions, average bond lengths, average bond population around the substitute atoms, average net charges and average dipole moments of different ion doped TiO_2 by geometry optimizing.

	E_f/eV	bond length/Å			net charge/eV				Dipole moment/D	ΔV /Å^3
		Ti–O	Ti–N	Pr–O	Ti	O	N	Pr	TiO_6	
pure TiO_2		1.9326			1.270	–0.630			0.0000	
N-doped	2.062	1.9350	1.9654		1.248	–0.633	–0.580		0.0400	0.064
Pr-doped	2.971	1.9404		2.1391	1.218	–0.623		1.670	0.0524	1.033
N+Pr-doped	4.083	1.9471	1.8821	2.0929	1.208	–0.590	–0.660	1.590	0.0984	1.035

3.2. Electronic structure and optical properties

In order to conveniently compare the electronic structures of different ions doping models, we set the same K-point mesh to sample the first Brillouim zone for all models. The calculated band gap of pure anatase TiO_2 is 2.54 eV, as shown in Fig. 2(a), it is less than the experimental value $E_g = 3.23$ eV due to the limitation of DFT: the discontinuity in the exchange–correlation potential is not taken into account within the framework of DFT.[18] The calculated band structures and partial density of states (PDOS) of N doping, Pr doping and N+Pr doping are displayed in Figs. 2(b)–2(d), respectively. If regardless the impurity energy levels, the band gaps are broadened to 2.56, 2.99 and 2.66 eV, respectively. For N-doped TiO_2, the PDOS calculation for the N 2p states shows three new impurity energy levels sitting above the top of VB. The results coincide with the recently calculated results.[19] For Pr-doped TiO_2, PDOS calculated Pr 4f states appear as seven isolated impurity energy levels located below the bottom of the conduction band (CB) with one of them completely occupied and the others unoccupied, these impurity energy levels sufficiently overlap with conduction band minimum (CBM) of TiO_2. For N+Pr-doped TiO_2, three N 2p bands are above the top of the VB. Simultaneously, there are seven Pr 4f bands located below the CBM, and the bands are smooth. This indicates that the locality of Pr 4f states is strong. N+Pr doping can further improve the separation of photoexcited carriers due to the formation of impurity energy levels.

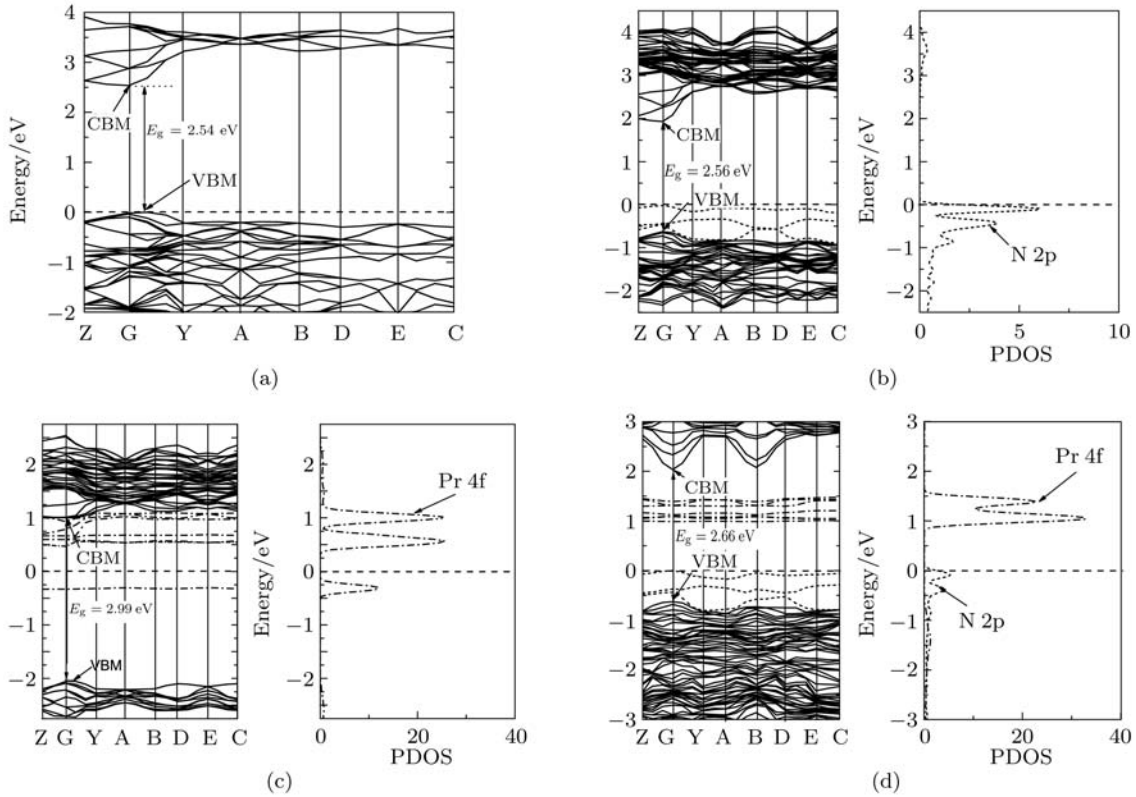


Fig. 2. Calculated band structures (left) and partial density of states (right) of (a) pure TiO_2, (b) N doped TiO_2, (c) Pr doped TiO_2, and (d) N+Pr doped TiO_2.

For further analysing the constitution of VB and CB and understanding the change of electronic structures, figure 3 shows the calculated PDOS and a comparison of the total density of states (TDOS) of pure TiO_2, N doping, Pr doping and N+Pr doping. The VB of pure TiO_2 located at –17.38∼–15.64 eV is mainly formed by O 2s states which are the intershell electrons, so the peak shape is sharp, and the locality is strong as shown in Fig. 3(a). The width of VB (–4.56∼0 eV) near the Fermi energy level is 4.56 eV, and the width of CB (2.54∼3.97 eV) is 1.43 eV. The VB and CB are formed mainly by the O 2p states

and Ti 3d states, and the former is dominated by O 2p states and the latter by Ti 3d states. The O 2p states and Ti 3d states show resonance phenomenon. This indicates that some covalence bond character between Ti and O atoms exist.[20] For N doping, the N 2p states are somewhat delocalized. It is clear that the CB of N-doped TiO_2 is consisted mainly by Ti 3d states, the VB is formed mainly by the O 2p states, and the impurity energy levels located above the top of VB are formed by hybridization of O 2p states and Ti 3d states with N 2p states, which coincide with the calculated results of Xu *et al.*[21] If the impurity energy levels are taken into account, the CBM is located at 1.93 eV, the width of VB (–5.16 eV∼–0.02 eV) is 5.14 eV. Compared with that of pure TiO_2, the band gap of N-doped TiO_2 narrowed to 1.95 eV, due to the mixing of N 2p states with O 2p states and Ti 3d which makes the width of VB broader. These kinds of impurity energy levels could act as acceptor levels, which can reduce the recombination rate of charge carriers and thus improve the photocatalytic activity of TiO_2. For Pr-doped TiO_2, the VB is also dominated mainly by O 2p states and the CB is by Ti 3d states. The impurity energy levels sufficiently mixed with the CBM are located below the bottom of VB, which are consisted by Pr 4f states. If this effect is considered, the width of VB is 4.55 eV, and that of CB is broadened to 2.07 eV, and the band gap is narrowed to 2.53 eV. As the shallow donor, these kinds of impurity energy levels could act as trap centre for the photoexcited electrons. It should be noted that, the PDOS of Pr atom near the Fermi energy is mainly formed by its 4f states. Pr 4f states make some contribution to making bond. Pr 4f states near the Fermi energy are rather sharp. This implies that the electrons from Pr 4f states are locality and not contribution much to making bond. This can be expressed by the Mulliken population analysis shown in Table 2. The bond populations as the judgment of bond strength give the distribution of electronic population among the atoms.[22] The high value of bond population shows that the bond is covalent, and the opposite is ionic.[23,24] The increased value of bond population shows the stronger covalency of bond. For Pr-doped TiO_2, when one Ti atom is substituted by Pr atom, six Pr–O bonds are formed. As shown in Table 2, compared with the bond population of bond Ti–O (0.3467) in pure TiO_2, the bond population value of bond Pr–O (0.1967) is lower, so bond overlap population between Pr and O is much smaller than that between Ti and O. This indicates the weaker covalency of bond Pr–O. For N+Pr-doped TiO_2, the formation of impurity energy levels located on the top of the VB is mainly contributed by hybridization of O 2p states, Ti 3d states with N 2p states. Simultaneously, the formation of impurity energy levels located below the CBM is mainly contributed by Pr 4f states. However, for the impurity energy levels sitting below the CBM, very high impurity doping concentration might form a recombination centre for photoexcited electron–hole pairs and result in a decrease in the quantum yield for the photocatalytic reaction. So we should control the Pr doping concentration severely in N+Pr-doped TiO_2. Regarding the impurity levels, the width of CB is 1.94 eV, the width of VB is 5.06 eV, and the band gap is narrowed to 1.09 eV. It should also be noted that the Pr 4f states are localized, but the DOS shape of Pr 4f states is smoother than that of Pr doping. This indicates that, compared with Pr doping, the Pr 4f states and O 2p states make stronger bond in codoped TiO_2. Table 2 shows that the net charge of Pr in Pr doping is 1.67 whereas that in N+Pr doping is 1.59. This suggests that Pr–O bond in Pr doping is more ionic than that in codoping. Bond overlap population between Pr and O in Pr doping is much smaller than that in codoping. Compared with the bond population value of bond Pr–O in Pr-doped TiO_2, the bond population value of bond Pr–O (0.2583) is higher. So the covalency of bond Pr–O is stronger in N+Pr doping. Figure 3(e) shows that the DOS shape of different ions doping becomes smoother and broader than that of pure TiO_2. This shows that the electronic nonlocality is more obvious owing to the reduction of crystal symmetry. For pure TiO_2, N doping, Pr doping and N+Pr doping, bond overlap population of Ti–O is 0.3467, 0.3468, 0.3520, 0.3486, respectively. This indicates that electronic nonlocality is more obvious, too.

On the basis of the electronic band structure, the optical absorption spectra of pure anatase TiO_2 between 300 nm and 800 nm are calculated. The results are shown in Fig. 4. For these calculations, the scissors operator applied is 0.69 eV, that accounts for the difference between the experimental band gap (3.23 eV) and the calculated band gap (2.54 eV). The value of absorption edge is at about 384 nm. Compared with pure TiO_2, we find that the fundamental absorption edges have red-shift toward visible-light region by N or Pr doping TiO_2. The reason is that the electrons in the VB can be excited to the impurity energy levels

and then subsequently excited to the CB by absorption of visible light due to the formation of impurity energy levels. The red-shift phenomenon is more obvious for N+Pr-doped TiO_2 than that of single doping, because the band gap of N+Pr-doped TiO_2 is the narrowest. So the optical absorption curve for N+Pr-doped TiO_2 shows the highest photoresponse under visible light.

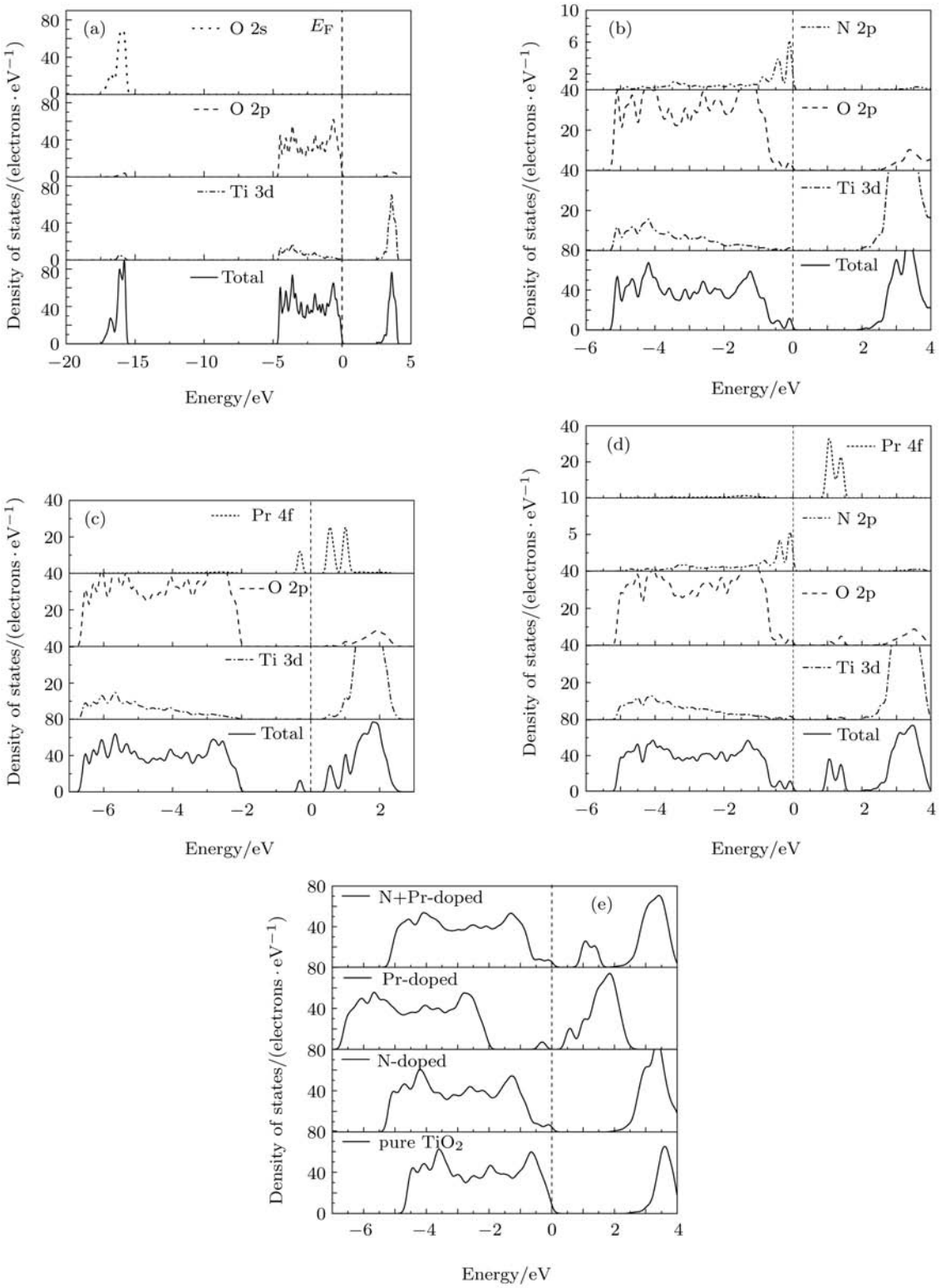


Fig. 3. Calculated PDOS of (a) pure TiO_2, (b) N-doped TiO_2, (c) Pr-doped TiO_2, (d) N+Pr-doped TiO_2, and (e) calculated and comparison TDOS of different ions-doped TiO_2.

Table 2. Mulliken population analysis of pure TiO_2, N-doped, Pr-doped and N+Pr-doped TiO_2.

		pure TiO_2		N-doped			Pr-doped			N+Pr-doped			
	species	Ti	O	Ti	O	N	Ti	O	Pr	Ti	O	N	Pr
atomic populations	Ion							1-6			1-6		
	charge/e	1.27	–0.63	1.26	–0.63	–0.58	1.22	–0.59	1.67	1.21	–0.55	–0.66	1.59
	Ti–O	0.3467			0.3468			0.3520			0.3486		
bond population	Ti-N				0.3933						0.4667		
	Pr–O							0.1967			0.2583		

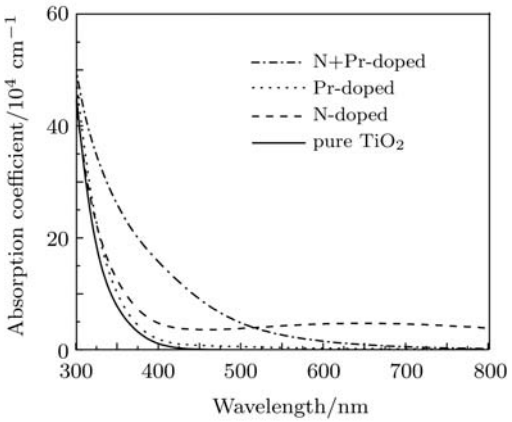


Fig. 4. The optical absorption curves calculated for various types ion-doped TiO_2.

3.3. Edge position

The ability of a semiconductor to undergo photoexcited electron transfer to adsorbed species on its surface is governed by its band energy position and the redox potentials of the adsorbate. The relevant potential level of the acceptor is thermodynamically required to be below (more positive than) the CB potential of the semiconductor. The potential level of the donor needs to be above (more negative than) the VB position of the semiconductor in order to donate an electron to the vacant hole.[25] In order to study the changes of the photocatalytic activity of different ion-doped TiO_2, we calculated the band edges position of N doping, Pr doping and N+Pr doping, respectively. The electronegativity of an atom here is the arithmetic mean of the atomic electron affinity and the first ionization energy, other than the common-defined term. The CB edge position of a semiconductor at the point of zero charge can be expressed empirically by:[26]

$$E_{\mathrm{CB}} = X - E^{\mathrm{e}} - 0.5E_{\mathrm{g}}, \qquad (2)$$

where E_{CB} is the CB edge potential, X is the electronegativity of the semiconductor which is the geometric mean of the electronegativity of the constituent atoms. E^{e} is the energy of free electrons on the hydrogen scale (≈4.5 eV), and E_{g} is the band gap energy of the semiconductor. From Eq. (2), the E_{CB} of TiO_2 is roughly –0.303 eV with respect to the normal hydrogen electrode. Subsequently the edge position of the VB of the photocatalyst is determined as 2.927 eV based on its band gap energy. This result is well consistent with the band energy position of TiO_2 in Ref. [25]. In Fig. 5, the band energy positions of different ion-doped TiO_2 were plotted and they have been changed little regardless of the impurity energy levels. It is well known that H_2O_2 and O_3 can oxide many organics because they have strong oxidative potential 1.77 eV (H_2O_2) and 2.07 eV (O_3).[26] Compared with them, N-doped and Pr-doped TiO_2 photocatalysts have excellent redox ability. However, if the impurity energy levels are considered, compared with that of pure TiO_2, the CB edge is slightly downward shifting, and the VB edge is slightly upper shifting for N+Pr-doped TiO_2. It means that the photocatalytic activity of N+Pr-doped TiO_2 is decreased. It is proved once again that we should control the doping concentration severely.

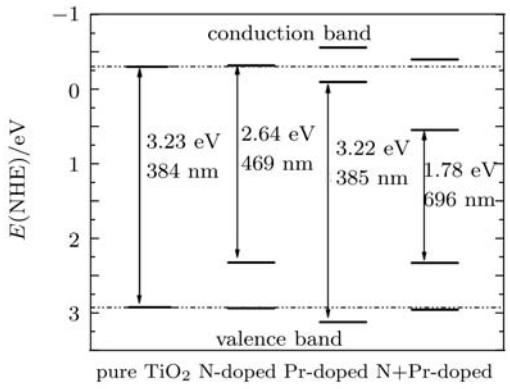


Fig. 5. The calculated band energy position of different ion-doped TiO_2. The band gaps and corresponding wavelength threshold were corrected by "scissors operator" in this figure.

3.4. Photocatalytic activity

Figure 6 shows the methyl blue (MB) degradation by P25, N–TiO_2, Pr–TiO_2 and N+Pr–TiO_2 (Pr:TiO_2 = 1 : 300 and 1 : 400 molar ratio) sintered at the same temperature at 500 °C, as well as P25. The results indicate that the N+Pr–TiO_2 catalyst demonstrates higher activity than that of P25, N–TiO_2 and Pr–TiO_2. The reason is that nitrogen doping narrows the band gap of TiO_2 to enhance visible light absorption. Simultaneously when one Ti atom is substituted by one Pr atom, the system will lose one electron. The surface of TiO_2 will absorb more OH^- to compensate for imbalance of the charge. So the OH^- on the surface can interact with the photoexcited holes, and produce free ·OH with strong oxidizing property. Thus, the photoexcited electrons and holes are separated more efficiently. The ·OH, as an active spice, is the central oxidant in the photocatalytic oxidation process. It can improve the photocatalytic activity. From Fig. 6, we can see that N+Pr–TiO_2 with Pr:TiO_2 = 1 : 400 has a better photocatalytic activity than that of Pr:TiO_2 = 1 : 300. This result indicates that lower Pr doping in N+Pr–TiO_2 is more beneficial to improve the photocatalytic activity, coincided with the above calculated results (The experimental results will be published in another paper).

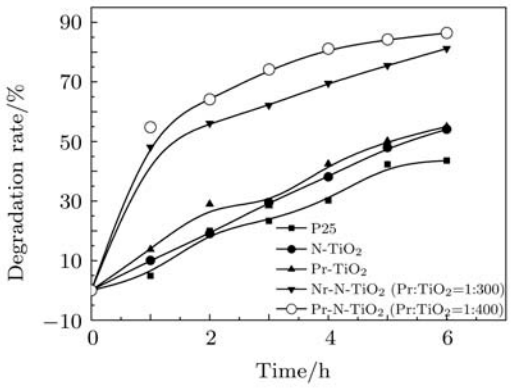


Fig. 6. Curves of MB degradation rate by the samples.

4. Conclusions

In this study, the crystal structures, electronic structure and optical properties of N-doped, Pr-doped and N+Pr-doped anatase TiO_2 were studied by using the plane-wave ultrasoft pseudopotential method based on the density functional theory. The calculations show that the dipole moments of octahedral in crystal are increased due to the change of lattice parameters, bond lengths and charges on atoms, which is very effective for the separation of photogenerated electron–hole pairs and the improvement of the photocatalytic activity of TiO_2. For N+Pr-doped TiO_2, the formation of impurity energy levels located below the CBM is mainly contributed by Pr 4f states, and the formation of impurity energy levels located on the top of the VB is mainly contributed by N 2p states. The formation of impurity energy levels can reduce the recombination rate of charge carriers and thus improve the photocatalytic activity of TiO_2. The narrowing of band gap results in the redshift of the fundamental absorption edges. According to the results of the band edge position, compared with that of pure TiO_2, for N+Pr-doped TiO_2, if regardless of impurity energy levels, the CB edge is upper shifting, and the VB edge is slightly downward shifting. This means that N+Pr-doped TiO_2 could maintain strong redox potentials of TiO_2. By measuring the photocatalytic activity of different samples, the experiment results show that the photocatalytic activity of codoping is obviously higher than that of the single ion doping. The experimental results accord with the calculated results.

Acknowledgments

The authors thank Zhao Zong-Yan for the helpful discussions and the High Performance Computer Centre of Yunnan University for providing software and hardware support in our calculations.

References

[1] Choi W, Termin A and Hoffmann M R 1994 *J. Phys. Chem.* **98** 13669
[2] Jing L Q, Sun X J, Xin B F, Wang B Q, Cai W M and Fu H G 2004 *J. Solid State Chem.* **177** 3375
[3] Asahi R, Morikawa T, Ohwakl T, Aoki K and Taga Y 2001 *Science* **293** 269
[4] Anpo M and Takeuchi M 2003 *J. Catal.* **216** 505
[5] Sukharev V and Kershaw R 1996 *J. Photochem. Photobiol.* A: *Chem.* **98** 165
[6] Jiang D, Xu Y, Hou B, Wu D and Sun Y H 2007 *J. Solid State Chem.* **180** 1787
[7] Shi J W, Zheng J T and Wu P 2009 *J. Hazard. Mater.* **161** 416
[8] Sasikala R, Sudarsan V, Sudakar C, Naik R, Sakuntala T and Bharadwaj S R 2008 *Int. J. Hydrogen Energ.* **33** 4966

[9] Xu J J, Ao Y H, Fu D G and Yuan C W 2008 *J. Colloid. Interface Sci.* **328** 447

[10] Liu Z Q, Zhou Y P, Li Z H, Wang Y C and Ge C C 2007 *Rare Metals* **26** 263

[11] Mi L, Xu P, Shen H and Wang P N 2007 *Appl. Phys. Lett.* **90** 171909

[12] Zhao Z Y and Liu Q J 2008 *Catal. Lett.* **124** 111

[13] Burdett J K, Hughbanks T, Miller G J, Richardson J W and Smith J V 1987 *J. Am. Chem. Soc.* **109** 3639

[14] Cui X Y, Medvedeva J E, Delley B, Freeman A J, Newman N and Stampfl C 2005 *Phys. Rev. Lett.* **95** 256404

[15] Sato J, Kobayashi H and Inoue Y 2003 *J. Phys. Chem.* B **107** 7970

[16] Ananpattarachai J, Kajitvidhyanukul P and Seraphin S 2009 *J. Hazard. Mater.* **168** 253

[17] Liang C H, Li F B, Liu C S, Lu J L and Wang X G 2008 *Dyes Pigments* **76** 477

[18] Perdew J P and Mel L 1983 *Phys. Rev. Lett.* **51** 1884

[19] Long M C, Cai W M, Wang Z P and Liu G Z 2006 *Chem. Phys. Lett.* **420** 71

[20] Yun J N and Zhang Z Y 2009 *Chin. Phys.* B **18** 2945

[21] Xu L, Tang C Q, Dai L, Tang D H and Ma X G 2007 *Acta Phys. Sin.* **56** 1048 (in Chinese)

[22] Mulliken R S 1955 *J. Chem. Phys.* **23** 1833

[23] Chen K, Fan G H, Zhang Y and Jing S F 2008 *Acta Phys. Sin.* **57** 3138 (in Chinese)

[24] Jin Y L, Lou S Y, Kong D G, Li W C and Du Z L 2006 *Acta Phys. Sin.* **55** 4809 (in Chinese)

[25] Linsebigler A L, Lu G Q and Yates J T 1995 *Chem. Rev.* **95** 735

[26] Tang J W and Ye J H 2005 *Chem. Phys. Lett.* **410** 104